Higher harmonics increase LISA's mass reach for supermassive black holes

K. G. Arun, Bala R. Iyer, B. S. Sathyaprakash, Siddhartha Sinha

Higher harmonics increase LISA's mass reach for supermassive black holes

K. G. Arun,[1,2,3,*] Bala R. Iyer,[1,†] B. S. Sathyaprakash,[4,‡] and Siddhartha Sinha[1,5,§]

[1]*Raman Research Institute, Bangalore, 560 080, India*
[2]*LAL, Univ Paris-Sud, IN2P3/CNRS, Orsay, France*
[3]*$\mathcal{GR}\varepsilon\mathbb{C}\mathcal{O}$, Institut d'Astrophysique de Paris—C.N.R.S., Paris, France*
[4]*School of Physics and Astronomy, Cardiff University, 5, The Parade, Cardiff, United Kingdom, CF24 3YB*
[5]*Deptartment of Physics, Indian Institute of Science, Bangalore, 560 012, India*

(Received 9 April 2007; published 1 June 2007)

Current expectations on the signal-to-noise ratios and masses of supermassive black holes which the Laser Interferometer Space Antenna (LISA) can observe are based on using in matched filtering only the dominant harmonic of the inspiral waveform at twice the orbital frequency. Other harmonics will affect the signal-to-noise ratio of systems currently believed to be observable by LISA. More significantly, inclusion of other harmonics in our matched filters would mean that more massive systems that were previously thought to be *not* visible in LISA should be detectable with reasonable SNRs. Our estimates show that we should be able to significantly increase the mass reach of LISA and observe the more commonly occurring supermassive black holes of masses $\sim 10^8 M_\odot$. More specifically, with the inclusion of all known harmonics LISA will be able to observe even supermassive black hole coalescences with total mass $\sim 10^8 M_\odot (10^9 M_\odot)$ (and mass ratio 0.1) for a low frequency cutoff of 10^{-4} Hz (10^{-5} Hz) with an SNR up to ~ 60 (~ 30) at a distance of 3 Gpc. This is important from the astrophysical viewpoint since observational evidence for the existence of black holes in this mass range is quite strong and binaries containing such supermassive black holes will be inaccessible to LISA if one uses as detection templates only the dominant harmonic.

DOI: 10.1103/PhysRevD.75.124002 PACS numbers: 04.30.Db, 04.25.Nx, 04.80.Nn, 95.55.Ym

I. INTRODUCTION

A. Supermassive black hole binaries and LISA

There is strong observational evidence for the existence of supermassive black holes (SMBHs) with masses in the range of $10^6 M_\odot$–$10^9 M_\odot$ (see e.g. Ref. [1] and references therein) in most galactic nuclei [2]. Therefore, mergers of galaxies, as evidenced by high-redshift surveys, should give rise to binaries containing SMBHs. Late stage evolution of a SMBH binary is dictated by the emission of gravitational radiation. The resulting loss of orbital energy and angular momentum would lead to the coalescence of the two holes. Indeed, x-ray observations have revealed the existence of at least one such system that would coalesce within the Hubble time [3]. Gravitational waves (GW) emitted in the process could be detected by the planned Laser Interferometer Space Antenna (LISA) [4].

Observation of SMBH binaries at high redshifts is one of the major science goals of LISA. These observations will allow us to probe the evolution of SMBHs and structure formation [5] and provide a unique opportunity to test general relativity (and its alternatives) in the strong field regime of the theory [6–10]. Observing SMBH coalescences with high (100–1000) SNR [8,9] is crucial for performing all the aforementioned tests.

*Electronic address: arun@lal.in2p3.fr
†Electronic address: bri@rri.res.in
‡Electronic address: B.S.Sathyaprakash@astro.cf.ac.uk
§Electronic address: p_siddhartha@rri.res.in

B. Restricted vs full waveforms as search templates in LISA

Motivated by the fact that matched filtering is more sensitive to the phase of the signal than its amplitude [11], search algorithms so far have deployed a waveform model involving only the *dominant harmonic* (at twice the orbital frequency), although the phase evolution itself is included to the maximum available post-Newtonian (PN) order (currently 3.5 PN, for nonspinning systems [12,13]). Waveforms in which all *amplitude* corrections are neglected, but the *phase* is treated to the maximum available order, are called *restricted waveforms* (RWF) and these are what are used so far in the analysis of data from ground-based detectors [14–17]. This paper will consider the advantage of using the *full waveforms* (FWF) in the context of LISA.

LISA is designed to detect gravitational waves in the frequency band 0.1–100 mHz. This frequency range determines the range of masses accessible to LISA because the inspiral signal would end when the system's orbital frequency reaches the mass-dependent last stable orbit (LSO). In the test-mass approximation, the angular velocity $\omega_{\rm LSO}$ at LSO is given by $\omega_{\rm LSO} = 6^{-3/2} M^{-1}$, where M is the total mass of the binary. Search templates that contain only the dominant harmonic cannot extract power in the signal beyond $f_{\rm LSO} = \omega_{\rm LSO}/\pi \simeq 4.39 (M/10^6 M_\odot)^{-1}$ mHz. This further implies that the frequency range [0.1, 100] mHz corresponds to the range $\sim 4.39 \times [10^4, 10^7] M_\odot$ for the total mass of binary black holes that would be accessible

to LISA.[1] However, as Table 1 of Ref. [1] would reveal, there is observational evidence for the existence of many SMBHs whose masses are of the order of 10^8–$10^9 M_\odot$. LISA will be *unable* to observe binaries containing SMBHs in this mass range if it used as search templates waveforms containing *only* the dominant harmonic.

Inclusion of higher-order amplitude terms in the waveform introduces the following two new features: (i) appearance of higher harmonics of the orbital phase and (ii) PN amplitude corrections to the leading as well as higher harmonics of the orbital frequency. For example, at 0.5 PN order, which is the first-order correction, there are two new harmonics Ψ and 3Ψ, where Ψ is related to the orbital phase of the binary as in Refs. [18,19]. More interestingly, in the expressions for the ''plus'' and ''cross'' polarizations, all odd harmonics of the orbital frequency are proportional to $\frac{\delta m}{M}$, where δm is the difference in the masses of the binary components (see Eqs. (5.7)-(5.10) of Refs. [19]). Another important feature of the full waveform is that the $(2n + 2)$th harmonic first appears at the nth PN order in the amplitude.[2] For example, the fourth harmonic first appears at 1 PN, and has PN amplitude corrections to its dominant term at 2 PN and 2.5 PN (see Refs. [18,19] for details).

Early investigations on the importance of amplitude corrections to search templates were carried out by Sintes and Vecchio [20,21]. Their study used only the first-order correction at 0.5 PN order. They concluded that the addition of the amplitude terms in the waveform did not improve the accuracy in the estimation of the source's angular position and the distance, whereas the estimation of the chirp and reduced masses could be 10 times better when compared to the RWF. Recently, in the context of ground-based detectors, Van Den Broeck and Sengupta [22–24] examined the implications of going beyond the restricted PN approximation and employing instead the full waveform [18,19]. The two main implications of the comprehensive analysis in Refs. [22,23] for terrestrial GW detectors may be summarized as follows:

(1) For binary neutron stars and stellar mass black holes, restricted waveforms overestimate the SNR as compared to the full waveform.
(2) The use of the full waveforms significantly increases the mass reach of second and third generation detectors, advanced LIGO and EGO being able to observe systems with total mass $\sim 400 M_\odot$, and a third generation detector as high as $10^3 M_\odot$.

In the present paper, we study in the context of LISA the implication of using templates based on the FWF (i.e. including *all* known harmonics of the orbital phase and *all* known amplitude corrections in the GW polarizations). Coalescences of SMBH binaries with masses $\sim 10^{8-9} M_\odot$ will *not* be observable by LISA if one uses only templates based on the RWF. Using templates based on amplitude-corrected full waveforms, instead of the usual restricted waveforms, will enable LISA to observe coalescences of SMBH binaries with total mass $\sim 10^8 M_\odot$ ($10^9 M_\odot$) if the lower frequency cutoff LISA can achieve is $\sim 10^{-4}$ Hz (10^{-5} Hz).

The rest of this paper is organized as follows: In Sec. II, we give the FWF in the frequency domain, by taking into account the orbital motion of LISA around the sun and its changing orientation. Section III discusses the results of our investigations where we compare the performances of the amplitude-corrected waveforms at different PN orders in terms of their mass reach and distance reach and correlate it to the ''observed'' spectrum in LISA. Section V concludes with a brief summary of the main results and assumptions underlying their derivation.

II. TEMPLATE WAVEFORMS FOR LISA

A. Amplitude-corrected waveform

For nonspinning binaries in quasicircular orbits inspiralling due to radiation reaction, waveforms were computed in Refs. [18,19] up to 2.5 PN order in amplitude and 3.5 PN in phase [12,13]. This waveform $h(t)$ is a linear combination of sine and cosine functions of multiples of the orbital phase $\Psi(t)$. The expression for the 2.5 PN polarization contains the first seven harmonics of the orbital phase, the dominant harmonic being the one at twice the orbital phase. The signal depends on the following parameters: D_L, the luminosity distance to the binary, m the total (redshifted) mass, ν the symmetric mass ratio (reduced mass divided by total mass), the spherical polar angles (θ, ϕ) determining the direction of the ''line of sight,'' the inclination angle ι of the angular momentum $\mathbf{L}$ of the binary with respect to the line of sight, and the polarization angle ψ which determines the orientation of the projection of $\mathbf{L}$ in the plane normal to the line of sight.

We rewrite the waveform in terms of only cosines in a form similar to [23]:

$$h(t) = \frac{2M\nu}{D_L} \sum_{k=1}^{7} \sum_{n=0}^{5} A_{(k,n/2)} \cos[k\Psi(t) + \phi_{(k,n/2)}] x^{(n/2)+1}(t), \tag{2.1}$$

where the coefficients $A_{(k,n/2)}$ and $\phi_{(k,n/2)}$ are functions of $(\nu, \theta, \phi, \psi, \iota)$, and $x(t) = (2\pi M F(t))^{2/3}$ is the post-Newtonian parameter with $F(t)$ the instantaneous *orbital* frequency. Terms $\frac{2M\nu}{D_L} x^{n/2+1}(t) A_{(k,n/2)}$ and $\phi_{(k,n/2)}$ are the wave amplitude and polarization phase, respectively, corresponding to the kth harmonic and $(n/2)$th PN order. We call the coefficients $A_{(k,n/2)}$ the polarization amplitudes.

[1] Although, binaries lighter than $10^4 M_\odot$ would, in principle, evolve through the LISA band they would not be luminous enough to be visible in LISA unless they are close by.

[2] The 0.5 PN term is an exception to this and also introduces a harmonic at the orbital frequency apart from the one at thrice the orbital frequency.

The orbital phase $\Psi(t)$ is a PN series in x, which, in the case of nonspinning binaries, is known to 3.5 PN order [12,13]. For a nonspinning source and a detector whose position and orientation are almost constant during the time of observation of the signal, all the above-mentioned angles are constants. For ground-based GW detectors dealt with in Refs. [22,23], one is in this situation.

B. Amplitude-corrected waveform including modulations due to LISA's orbital motion—Time domain

LISA will be able to observe many sources from their early stages of inspiral and most would last for a pretty long time. We shall only consider binary sources that last for a year or less before the merger. Since the LISA plane is tilted by 60° with respect to the plane of the ecliptic, during the course of its heliocentric orbit its orientation and position varies periodically, with a period of 1 yr and the signal in Eq. (2.1) will suffer additional amplitude and phase modulations. Thus in the case of LISA the angles θ, ϕ, and ψ (but not ι) appearing in Eq. (2.1) are functions of time. To proceed further, in the frame of a nonrotating observer fixed to the solar system barycenter, we denote by the location of the source on the sky by the spherical polar angles θ_S and ϕ_S and the orientation of the source by the spherical polar angles θ_L and ϕ_L determining the direction of the orbital angular momentum $\mathbf{L}$ of the binary. The transformation between the fixed set of angles[3] $(\theta_S, \phi_S, \theta_L, \phi_L)$ and the time-dependent angular coordinates of the source $(\theta(t), \phi(t), \psi(t), \iota)$ as measured by LISA are given in Ref. [25].

Generalizing, Ref. [25] from the RWF to the FWF, the signal as seen in LISA is of the form,

$$h(t) = \frac{\sqrt{3}}{2}\frac{2M\nu}{D_L}\sum_{k=1}^{7}\sum_{n=0}^{5} A_{(k,n/2)}(t)\cos[k\Psi(t) + \phi_{(k,n/2)}(t) + k\phi_D(t)]x^{(n/2)+1}(t). \tag{2.2}$$

The PN parameter $x(t)$ appearing in Eq. (2.2) is still equal to $(2\pi MF(t))^{2/3}$, where $F(t)$, however, is the orbital frequency as measured by a *nonrotating observer located at the solar system barycenter*. The term $\phi_D(t)$ is the *Doppler phase* [25], accounting for the phase difference of the gravitational wave front between LISA and the solar system barycenter. The time dependence of $\phi_D(t)$ is due to the orbital motion of LISA about the barycenter. It is given by

$$\phi_D(t) = 2\pi F(t) R \sin\theta_S \cos[\phi(t) - \phi_S], \tag{2.3}$$

where $R = 1$ AU and $\phi(t)$ is the angular position of LISA with respect to the barycenter given by $\phi(t) = 2\pi\frac{t}{T}$, T being equal to 1 yr.

[3]This is a different notation from [25], where the source angles measured in the fixed barycenter frame are denoted by $(\bar{\theta}_S, \bar{\phi}_S, \bar{\theta}_L, \bar{\phi}_L)$

C. Amplitude-corrected waveform including modulations due to LISA's orbit—Frequency domain

The above waveform is valid in the adiabatic regime, where the radiation-reaction time scale is much larger than the orbital time scale. We also note that the additional amplitude and Doppler modulations in the waveform for LISA vary on time scales of 1 yr (i.e. $\sim 3 \times 10^7$ s), while LISA can observe orbital periods at most up to 2×10^5 s, (i.e. gravitational wave frequencies of order 10^{-5} Hz). Consequently, the Doppler modulations change much more slowly (a hundredth) than the orbital phase. This permits the use of the stationary phase approximation (SPA) to obtain an analytical form for the Fourier transform (FT) $\tilde{h}(f)$ of the signal:

$$\tilde{h}(f) \simeq \frac{\sqrt{3}}{2}\frac{2M\nu}{D_L}\sum_{k=1}^{7}\sum_{n=0}^{5} \times \frac{A_{(k,n/2)}(t(f/k))x^{(n/2)+1}(t(f/k))e^{-i\phi_{(k,n/2)}(t(f/k))}}{2\sqrt{k\dot{F}(t(f/k))}} \times \exp[i\psi_f(t(f/k))], \tag{2.4}$$

where an overdot denotes derivative with respect to time and $\psi_f(t(f/k))$ is given by

$$\psi_f(t(f/k)) = 2\pi f t(f/k) - k\Psi(t(f/k)) - k\phi_D(t(f/k)) - \pi/4. \tag{2.5}$$

The PN expansions for $t(F)$, $\Psi(F)$, $\dot{F}(F)$ are given in Ref. [12]. The expression in Eq. (2.4) within the summation over k represents the FT due to the kth harmonic. It should be noted that the term $\dot{F}$ may be treated in different ways that could lead to numerically different results. In a numerical treatment, for instance, one could avoid performing a further reexpansion. Alternatively, one could reexpand the denominator in the amplitude and truncate the resulting expression at the nth PN order, to obtain the nPN amplitude-corrected waveform. References [22,23] choose the latter and we follow them in this work.

Radiation reaction results in an increase in the orbital frequency $F(t)$ which will ultimately drive the system beyond the adiabatic inspiral phase and the inspiral waveform given above will no longer be valid. In the first approximation this is expected to occur when the orbital frequency $F(t)$ reaches $F_{\rm LSO}$—the orbital frequency of the LSO of a Schwarzschild solution with the same mass as the binary's total mass M,

$$F_{\rm LSO} = (2\pi 6^{3/2} M)^{-1}. \tag{2.6}$$

Thus, we truncate the signal in the time domain at a time $t_{\rm LSO}$, given implicitly by $F(t_{\rm LSO}) = F_{\rm LSO}$. In the SPA, the main contribution to the FT of the kth harmonic at a given Fourier frequency f, comes from the neighborhood of the time when the instantaneous value of the kth harmonic sweeps past f. Thus the kth harmonic is not expected to

contribute significant power to the FT for frequencies above $kF_{\rm LSO}$, if the signal is truncated in the time domain beyond $t_{\rm LSO}$. This motivates the truncation of the FT due to the kth harmonic at frequencies above $kF_{\rm LSO}$ by a step function $\theta(kF_{\rm LSO} - f)$ [$\theta(x) = 1$, for $x \geq 0$, and 0 for negative x].

III. SIGNAL-TO-NOISE RATIOS IN LISA WITH HIGHER HARMONICS

In this section we investigate the effect of the higher harmonics in LISA observations of supermassive black hole binaries. The LISA waveform discussed in the previous section will be used for the analysis.

Given a waveform h, the best signal-to-noise ratio (SNR) achieved using an optimal filter is given by $\rho[h] \equiv (h|h)^{1/2}$, where $(.|.)$ is the usual inner product in terms of the one-sided noise power spectral density $S_h(f)$ of the detector. With the convention for Fourier transforms, $\tilde{x}(f) = \int_{-\infty}^{\infty} x(t) \exp(-2\pi i f t) dt$, the inner product is given by:

$$(x|y) \equiv 4 \int_{f_s}^{f_{\rm end}} \frac{{\rm Re}[\tilde{x}^*(f)\tilde{y}(f)]}{S_h(f)} df. \tag{3.1}$$

For an optimal filter, which maximizes the overlap of the signal with template, one can write

$$\rho^2 = 4 \int_{f_s}^{f_{\rm end}} \frac{|\tilde{h}(f)|^2}{S_h(f)} df. \tag{3.2}$$

We use the non-sky-averaged noise-spectral density as given in Eqs. (2.28)–(2.32) of Ref. [6].

A. Choice of frequency cutoffs $f_{\rm end}$, $f_{\rm s}$

The upper limit of integration $f_{\rm end}$ is taken to be the minimum of 7 $F_{\rm LSO}$ and 1 Hz, the latter being a conventional upper cutoff for the LISA noise curve. The lower limit $f_{\rm s}$ is chosen assuming LISA observes the inspiral for a duration $\Delta t_{\rm obs}$ before it reaches the LSO. Using the quadrupole formula, we find that the orbital frequency at the epoch $t_{\rm LSO} - \Delta t_{\rm obs}$ is given by

$$F(t_{\rm LSO} - \Delta t_{\rm obs}) = \frac{F_{\rm LSO}}{(1 + \frac{256\nu}{5M} \Delta t_{\rm obs} v_{\rm LSO}^8)^{3/8}}, \tag{3.3}$$

where $v_{\rm LSO}$ is the orbital velocity and $t_{\rm LSO}$ the epoch at which the orbital frequency reaches the value $F_{\rm LSO}$. We take $v_{\rm LSO} = 1/\sqrt{6}$, the orbital velocity at the LSO in the case of a test mass orbiting a Schwarzschild black hole. We designate $F(t_{\rm LSO} - \Delta t_{\rm obs})$ as $F_{\rm in}$. Thus the kth harmonic will have a frequency $kF_{\rm in}$, $\Delta t_{\rm obs}$ before $t_{\rm LSO}$. The above formula reduces to the simpler form in Ref. [6] as $v_{\rm LSO} \to \infty$. For the mass values explored in this work there is no significant dependence of the results on this choice. In all our calculations we take $\Delta t_{\rm obs}$ to be 1 yr.

The lower cutoff for the kth harmonic should be the maximum of the lower cutoff of LISA (10^{-4} Hz) and $kF_{\rm in}$ and simply implemented by truncating the waveform due to the kth harmonic by another step function $\theta(f - kF_{\rm in})$ and choosing $f_{\rm s}$ to be 10^{-4} Hz. It is worth noting that the kth harmonic probes a larger interval of the frequency domain i.e. $k(F_{\rm LSO} - F_{\rm in})$ relative to the fundamental harmonic. For brevity, we refer to this as the span of the kth harmonic.

There is a caveat with regard to the use of higher harmonics that is worth mentioning: In the time domain the waveform should begin when the highest harmonic reaches the lower cutoff. This has an implication on data analysis as the templates will be an order of magnitude longer than before. Thus, it might be sensible to use higher harmonics only in the case of higher masses.

B. Observed signal spectrum with LISA

To get some insight into the effect of higher harmonics via amplitude corrections let us first look at the SNR integrand, i.e., the ''noise-weighted signal power'' per unit logarithmic frequency interval [26]. Rewriting the expression for the SNR as

$$\rho^2 = 4 \int_{f_s}^{f_{\rm end}} \frac{f|\tilde{h}(f)|^2}{S_h(f)} d\ln(f), \tag{3.4}$$

the quantity of our interest is

$$\mathcal{P}(f) \equiv \frac{d(\rho^2)}{d(\ln f)} = \frac{f|\tilde{h}(f)|^2}{S_h(f)}, \tag{3.5}$$

which is designated as the ''observed spectrum,'' following [24]. The observed spectrum is plotted versus frequency for given masses in Fig. 1. As is the case for ground-based detectors [24], the spectrum due to the FWF has a lot more structure and is highly oscillatory because of interference between various harmonics. For the $(10^5, 10^6)M_\odot$ system, the mass being low, the second harmonic and hence the RWF extends up to frequencies $\sim 2 \times 10^{-3}$ Hz, where LISA is most sensitive. This leads to a rapid increase in the observed spectrum in this frequency region. The spectrum due to the FWF, containing higher harmonics continue beyond the RWF into the most sensitive part of the LISA band. For the $2(10^6, 10^7)M_\odot$ system, the frequency span of the second harmonic is small and the sensitive region of the LISA band lies beyond its maximum reach.

IV. THE EFFECT OF HIGHER HARMONICS

Following the analysis of Refs. [22,23], we classify the sources into two types: In the first category are sources for which the dominant (second) harmonic has a large frequency span in the LISA band. The second category on the other hand comprise sources whose dominant harmonic *fails* to enter the LISA bandwidth but the higher harmonics *do*. Since the upper cutoff frequency for each harmonic is inversely proportional to the total mass (from the expression for $F_{\rm LSO}$), we note that the sources of the first type will

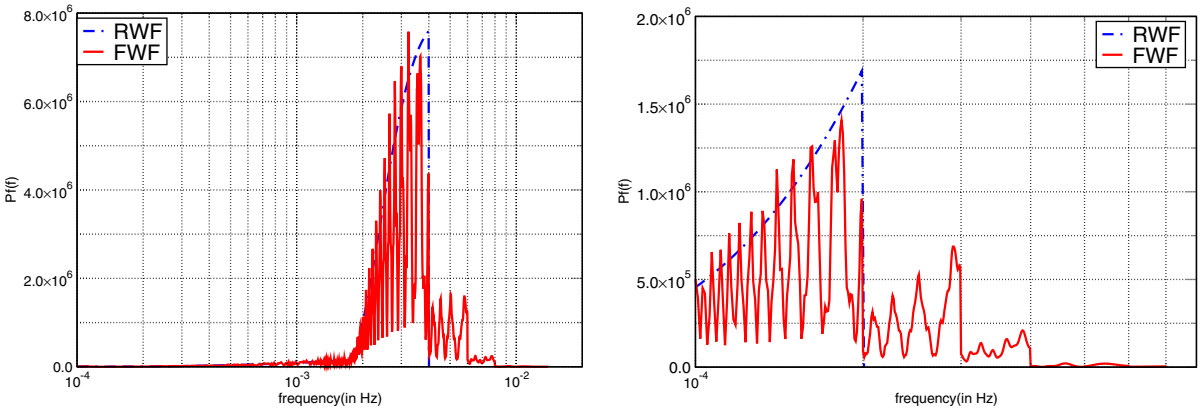

FIG. 1 (color online). The observed spectrum, $\mathcal{P}(f) \equiv \frac{d(\rho^2)}{d(\ln f)} = \frac{f|\tilde{h}(f)|^2}{S_h(f)}$, in LISA using the full (solid lines) and restricted (dashed lines) waveforms, for two archetypal binaries, $(10^5, 10^6)M_\odot$ (left) and $2 \times (10^6, 10^7)M_\odot$ (right). The sources are assumed to be at 3 Gpc and their orientation with respect to the solar system barycenter is chosen to be $\theta_S = \cos^{-1}(-0.6)$, $\phi_S = 1$, $\theta_L = \cos^{-1}(0.2)$, $\phi_L = 3$. The spectrum is much more complicated and highly oscillatory for the FWF than for the RWF, because of interference between various harmonics. The higher frequency reach of the FWF is due to the presence of higher harmonics as apparent in the figure. The spectrum for the system in the left panel sharply rises at a frequency $\sim 2 \times 10^{-3}$ Hz. Beyond this frequency, the effective LISA noise decreases sharply with increasing frequency (as there are fewer galactic binaries per frequency bin) leading to the observed increase in the spectrum.

have total mass less than some value which we call the RWF mass reach, the maximum mass detectable by the RWF, while the second type will have masses greater than this value. The condition that the upper cutoff of the dominant harmonic is less than or equal to the lower cutoff of LISA (i.e., by the inequality $2F_{\rm LSO} \leq f_s$) determines the RWF mass reach. The choice of f_s for the LISA mission is still not clear and theoretical implications of this choice are explored in e.g. Ref. [27]. For f_s in the range $[10^{-5}, 10^{-4}]$ Hz the RWF mass reach varies over the range $[4.39, 43.9] \times 10^7 M_\odot$, the lower end of the mass range corresponding to the higher end of the frequency range.

A. How higher harmonics affect signal visibility

In Fig. 2 we plot the SNRs computed using the RWF and FWF as a function of the binary's total mass for two values of the mass ratio.[4] We first consider systems whose total mass is less than $4 \times 10^7 M_\odot$. For these systems, the SNRs computed using the two different approximations agree with each other to within 10%, with the RWF overestimating the SNR, when compared to the FWF, in most of the range. This is explicitly shown for a $(10^6, 10^7)M_\odot$ binary in the first column of Table I. Indeed, but for the slight increase in SNR as we go from 0 PN to 0.5 PN, we find a steady decrease as one increases the PN order of the amplitude correction.

The reduction in SNR at higher PN orders can be understood by studying the structure of $|\tilde{h}(f)|^2$, the numerator in the integrand of the SNR in Eq. (3.2). There are basically three types of terms:

(1) *direct* terms in which the phases in Eq. (2.4) cancel

$$A^2_{(k,n/2)}(t(f/k))f^{-7/3}(Mf)^{2n/3},$$

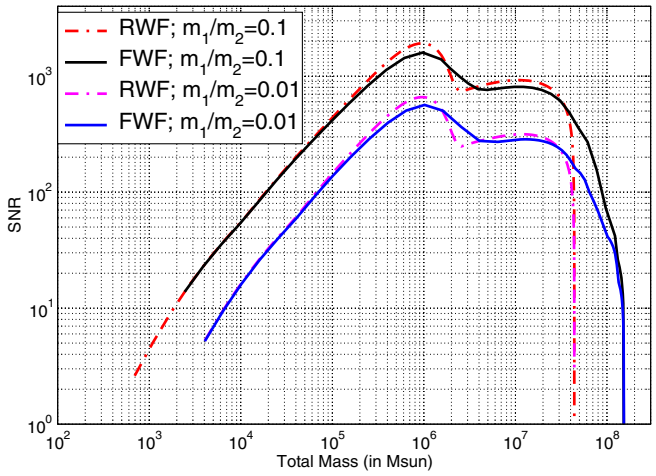

FIG. 2 (color online). SNR versus total mass for mass ratios of 0.1 and 0.01. The figure shows that apart from the dips due to white-dwarf confusion noise, for mass values where the RWF enters the LISA band, the corresponding SNR is consistently more than the SNR produced by the FWF. However, for mass values where the second harmonic terminates before it reaches the LISA bandwidth, the FWF which has higher harmonics that enter the LISA band produces significant SNRs. The frequency reach of a harmonic depends only on the total mass, and thus the mass reach of the FWF is independent of the mass ratio. For more asymmetric systems, the magnitude of the SNR is low for all masses both for the RWF and the FWF. Sources are at a luminosity distance of 3 Gpc with fixed angles given by $\theta_S = \cos^{-1}(-0.6)$, $\phi_S = 1$, $\theta_L = \cos^{-1}(0.2)$, $\phi_L = 3$.

[4]Our codes are calibrated by reproducing the results of [22,23], which considers ground-based detectors, and also of [28], which computes SNRs in LISA using RWF.

TABLE I. SNRs due to successive PN amplitude-corrected waveforms, with phase corrections to 3.5 PN order in all cases. The orientation of the source with respect to the solar system barycenter is chosen to be $\theta_S = \cos^{-1}(-0.6)$, $\phi_S = 1$, $\theta_L = \cos^{-1}(0.2)$, $\phi_L = 3$. For the $(10^6$–$10^7)M_\odot$ binary system, all harmonics enter deep into the sensitive part of the LISA bandwidth. Apart from an increase at 0.5 PN, we see a consistent reduction in the SNR on inclusion of higher PN order amplitude corrections. For the $(5.5 \times 10^6, 5.5 \times 10^7)M_\odot$ binary system, the second harmonic fails to enter the LISA bandwidth, while the third harmonic spans a small insensitive region. Thus the SNR due to the RWF is zero, while the SNR due to the 0.5 PN waveform is smaller than the SNRs due to higher-order PN terms. Both sources are at a distance of 3 Gpc.

PN order	SNR $(10^6$–$10^7)M_\odot$	$5.5 \times (10^6$–$10^7)M_\odot$
0	924.48	0
0.5	1025.8	211.98
1	928.48	343.17
1.5	869.78	319.34
2	824.65	266.65
2.5	809.51	277.34

(2) *interference* terms between *different* PN corrections of the *same* harmonic,

$$A_{(k,m/2)}(t(f/k))A_{(k,n/2)}(t(f/k))f^{-7/3}(Mf)^{(m+n)/3} \times \cos[\phi_{(k,m/2)}(t(f/k)) - \phi_{(k,n/2)}(t(f/k))],$$

(3) *harmonic mixtures*[5] which are terms containing the interference between *different* PN corrections of *different* harmonics, e.g. the $m/2$th PN correction of the kth harmonic and $n/2$th PN correction of the lth harmonic.

$$A_{(k,m/2)}(t(f/k))A_{(l,n/2)}(t(f/l))f^{-7/3}(Mf)^{(m+n)/3} \times \cos[\psi_f(t(f/k)) - \phi_{(k,m/2)}(t(f/k)) - \psi_f(t(f/l)) + \phi_{(l,n/2)}(t(f/l))],$$

where $\psi_f(t(f/k))$ is given by Eq. (2.5).

All these terms are scaled by $\mathcal{M}^{5/3}$, where $\mathcal{M} = M\nu^{3/5}$ is the chirp mass. (Additional multiplicative factors have been omitted in the above expressions, among which are the step functions mentioned earlier and PN expansion coefficients of the denominator of the Fourier amplitude in Eq. (2.4), the latter being time independent.)

[5]We use the term "harmonic mixtures" at the risk of being mistaken to the well-known "harmonic mixing" in music. Our use of the phrase "harmonic mixtures" is simply to convey the physical effect of the interference between different harmonics.

B. The effect of higher harmonics in ground-based detectors

Before we explain the SNR trends in the context of LISA, we mention that for ground-based detectors a similar effect was found in Ref. [23] for a different but corresponding mass region. The lower cutoff for a typical ground-based detector, say Advanced LIGO is 20 Hz, and the effect of higher harmonics is seen for masses less than $\sim 220M_\odot$. In that case, as mentioned earlier, the polarization amplitudes and phases are constants. The RWF contains only the Newtonian term of the second harmonic and thus $|\tilde{h}(f)|^2$ consists of a single direct term with $n = 0$ and $k = 2$.

With the inclusion of higher-order amplitude terms in the waveform, PN corrections to the dominant harmonic, and higher harmonics and their PN corrections, also contribute to the SNR. In other words, the signal power spectrum $|\tilde{h}(f)|^2$ will contain all three types of terms discussed before. From the form of the *direct terms*, it is evident that their contribution to the SNR will be positive definite. We also note that, for ground-based detectors, the frequency dependence of the *direct* and *interference* terms will just be a power law. However, the sign of the interference terms (and consequently their contribution to the SNR) depends on the difference between the polarization phases of different PN corrections for the same harmonic. Van Den Broeck and Sengupta showed that for a given harmonic, for all allowed values of the parameters $(\nu, \theta, \phi, \psi, \iota)$, each PN correction is almost "out of phase" with *both* the PN correction preceding and succeeding it.[6] The resulting negative terms (representing destructive interferences) reduce the SNR as one includes higher PN amplitude corrections in the waveform.

The third type of terms, harmonic mixtures, however, are highly oscillatory functions of the frequency, as the phase difference $\psi_f(t(f/k)) - \psi_f(t(f/l))$ between the kth and the lth harmonic become even or odd multiples of π. As one integrates over f, these oscillations tend to cancel out, and thus the contribution to the SNR from these terms are numerically much smaller relative to the first two types of terms.

C. Effect of higher harmonics for binaries with $M < 4 \times 10^7 M_\odot$

In the case of LISA, because of the polarization factors, the amplitudes of none of the three types of terms is a simple power law in f. The periodic variation of, for example, $A_{(2,0)}$ (period being 1 yr) appears as an amplitude modulation $A_{(2,0)}(t(f/2))$ in the Fourier transform, where the argument $t(f/2)$ of $A_{2,0}$ is given by

[6]Note, however, that Ref. [23], argues this in a somewhat different form.

$$t(f/2) = -\frac{5}{256\pi^{8/3}\mathcal{M}^{5/3}}\frac{1}{f^{8/3}} + \text{PN corrections.} \quad (4.1)$$

Hence, in the frequency domain $A_{(2,0)}$ will undergo one complete oscillation as f varies from $2F_{\rm in}$ (see Eq. (3.3)) to $2F_{\rm LSO}$. However, because of the *inverse* power-law dependence on f, the oscillation of $A_{(2,0)}$ is confined to a small frequency interval above $F_{\rm in}$ and remains fairly constant over a major portion of the frequency span $2(F_{\rm LSO} - F_{\rm in})$ (see Fig. 3). For masses higher than the one shown in Fig. 3, this region of significant variation moves to the left of the figure. On including in our analysis the effect of detector sensitivity (weighting down by $S_h(f)$) this variation of $A_{(2,0)}$ gets damped out when one evaluates the integral in Eq. (3.2). For masses satisfying $2F_{\rm in} \ll 10^{-4}$ Hz, the lower cutoff for LISA, this region of variation will fall below the LISA band.

The polarization phases determining the sign of the interference terms between the same harmonics also vary with f. However, as mentioned earlier, the phase relationships of the polarization phases are independent of the parameter values. Thus the modulations which change the values of $(\theta, \phi, \psi, \iota)$ do not affect the trend of reduction of SNR with amplitude corrections. The Doppler modulations, which appear in only harmonic mixtures, are also not important as far as SNR is concerned.

Finally, we would like to note an important point not explicitly mentioned in Ref. [23]. As the difference between the polarization phases of successive PN corrections of the same harmonic tend to be nearly π, alternate PN corrections necessarily interfere constructively. Hence there are positive contributions also from the interference terms. Now, the numerical value of the contribution to SNR from each of these terms depends on the magnitude of the polarization amplitude and the power of (Mf). It can be checked that for all allowed values of $(\nu, \theta, \phi, \psi, \iota)$, the polarization amplitudes are roughly of the same order in magnitude. Consider the Newtonian term of the dominant harmonic and its interference with the first two corrections at 1 PN and 1.5 PN. The Newtonian term will be out of phase with the 1 PN term, but in phase with the 1.5 PN one. The two corresponding interference terms will contain powers of $(Mf)^{2/3}$ and (Mf), respectively, and since they have the same frequency span, the absolute numerical value of the contribution to SNR from the former will be more since $(2\pi Mf)^{1/3}$ will always be less than $1/\sqrt{6}$. Numerical values of contributions from interference between higher PN corrections of the second harmonic successively decrease. The same argument applies for all the other harmonics, and thus, inclusion of amplitude corrections will lead to an overall reduction in SNR.

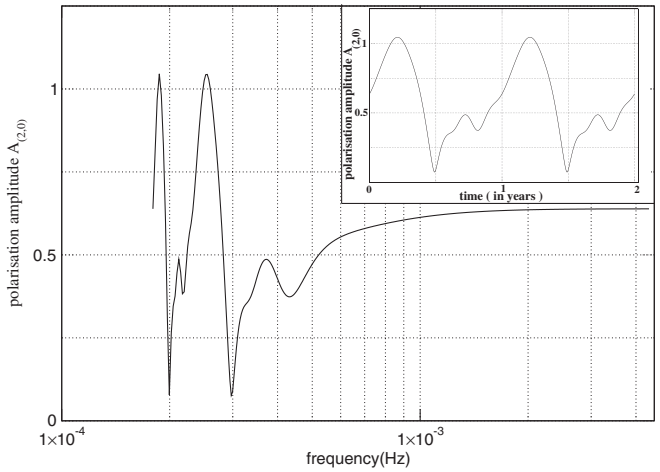

FIG. 3. Variation of polarization amplitude of the RWF with frequency and time (inset). The inset, plotted over a duration of two years clearly shows periodicity due to LISA's orbital motion around the Sun. The binary mass, $(10^6 - 10^4)M_\odot$, has been chosen such that it can, in principle, be observed for two years. The plot in the frequency domain shows that the variation of the polarization amplitude is confined to a very small part of the frequency span of the dominant harmonic, and essentially behaves as a constant in the frequency domain.

The first column of Table I clearly demonstrates the effect of higher harmonics on SNRs. The increase in SNR for the 0.5 PN waveform (with respect the RWF SNR) is also easily explained by noting that the 0.5 PN correction only adds (apart from harmonic mixtures) two direct terms to $|\tilde{h}(f)|^2$, corresponding to the first and third harmonics ($n = 1$, $n = 3$). Clearly, from the discussion in the previous subsection, the 0.5 PN waveform will have a higher SNR than the RWF, independent of the binary parameters.

For $10^3 \lesssim M \lesssim 10^5 M_\odot$, the difference between the RWF and the FWF is not visible on the scale of Fig. 2 because for this mass range all the direct and interference terms corresponding to harmonics higher than the dominant ones, which are scaled by higher powers of (Mf), are negligible.

D. Visibility of systems with $M > 4 \times 10^7 M_\odot$

In their analysis of the implications of the FWF for ground-based detectors Van Den Broeck and Sengupta [22,23] pointed out an interesting effect due to higher harmonics. An analogous effect is found in the case of LISA in spite of the additional amplitude and Doppler modulations that exist in this case.

Normally, the harmonic at twice the orbital frequency dominates the SNR. However, when the dominant harmonic fails to reach the LISA band the higher harmonics become important, which transpires for masses greater than $4 \times 10^7 M_\odot$. Even though the second harmonic falls below the lower cutoff f_s of the LISA bandwidth, the kth harmonic, $k > 2$, that has power up to a frequency $kF_{\rm LSO}$, might cross f_s and produce a significant SNR. Of course, the kth harmonic would fall below the LISA sensitivity band for masses which satisfy the equality $f_s = kF_{\rm LSO}$.

Thus, higher PN order waveforms, which bring in higher harmonics, are capable of producing a significant SNR, even when the RWF fails to produce any.

Let us examine this in a little more detail starting from the values of mass where the second harmonic dominates and the RWF is adequate. Eventually, for larger values of the total mass, the inequality $f_s \geq 3F_{\rm LSO}$ becomes true. Then the 0.5 PN waveform, which contains the first and the third harmonic, terminates before reaching f_s and consequently the SNR due to the 0.5 PN waveform goes to zero. SNRs for different PN waveforms for a binary whose dominant harmonic falls below f_s and the third harmonic has a small span in the LISA bandwidth is given in the second column of Table I. Note that for the $5.5(10^6$–$10^7)M_\odot$ system, the 1 PN waveform has a higher SNR than the 0.5 PN one. This is due to the absence of the first harmonic and the small span of the third harmonic in the LISA bandwidth. Further, the 2.5 PN waveform has a slightly larger SNR compared to 2 PN. This is due to the absence of the first and second harmonic and the small contribution from the third harmonic, all of which contribute interference terms due to their 2.5 PN corrections. However, this increase is marginal, and is not generic. We have explicitly checked by choosing different angles that there can be a small decrease also. The detailed results for LISA are summarized in Fig. 4. We see that for masses for which the 1 PN waveform fails to reach the LISA bandwidth, the higher PN order amplitudes are capable of producing SNRs as high as 100. Thus, the use of the FWF will enable LISA to make observations of SMBHs in the astrophysically interesting mass regime, which would not be possible had one used only the standard RWF.

Using the expression for $F_{\rm LSO}$, it is simple to argue that the mass reach for the 2.5 PN FWF, which has the seventh harmonic of the orbital frequency, is $7/2$ times the RWF (around $1.5 \times 10^8 M_\odot$). The above ratio, of course, depends on the assumption that the Schwarzschild (test-particle case) LSO frequency will not be very different from the LSO frequency in the comparable mass case.

We conclude with a discussion of a minor, but clear, feature seen in Fig. 2 for LISA, but not present for the ground-based detectors, concerning the relative values of the SNR obtained using the RWF and the FWF. For most of the mass range probed the RWF overestimates the SNR relative to the FWF; however, the figure clearly shows an anomaly for masses around $\sim 2 \times 10^6 M_\odot$. To understand this, we first note that the dips in the two curves in Fig. 2, are due to the bump in the LISA noise curve [6] just above 10^{-3} Hz. This bump is due to the domination of white-dwarf confusion noise over instrumental noise and lies just below the most sensitive frequency region ($\sim 3 \times 10^{-3}$ Hz $- 2 \times 10^{-2}$ Hz) of the LISA band. Below 3×10^{-3} Hz, the noise increases sharply till one reaches the bump. For binaries of mass greater than $1.5 \times 10^6 M_\odot$, the frequency span of the dominant harmonic ends just around the bump and the sensitive region of the LISA band is beyond the span of this harmonic. However, higher harmonics incorporated in the FWF are able to reach the sensitive part of the noise curve. This leads to higher SNR for the FWF relative to the RWF. This reversal of trend continues up to masses $4 \times 10^4 M_\odot$. Above this mass, the frequency span of the seventh harmonic ends before the sensitive region of the LISA band and the general trend is restored.

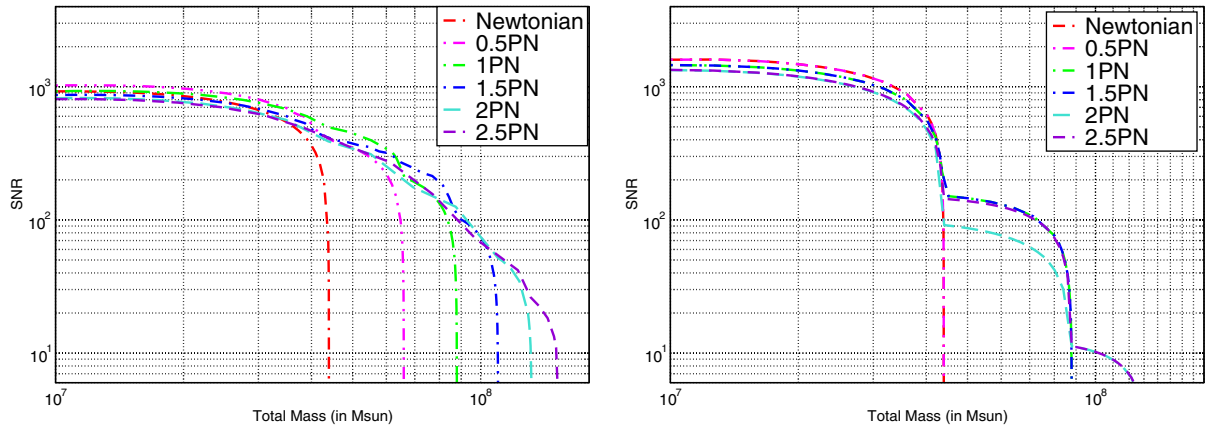

FIG. 4 (color online). SNR versus total mass for successive PN amplitude-corrected waveforms and 3.5 PN phasing. The left panel corresponds to a mass ratio of 0.1 while the right panel plots the same quantities for mass ratio of 1 (equal mass systems). The $(2n + 2)$th harmonic first appears at the nth PN order. For a binary of given total mass, the upper cutoff of the kth harmonic of the orbital frequency in the frequency domain is proportional to k and inversely proportional to the total mass. As the mass increases the upper cutoff for the 2nd harmonic falls below the lower cutoff of the LISA detector, leading to a zero value of SNR due to the RWF. The higher harmonics still enter the sensitive bandwidth of LISA and higher PN order waveforms produce significant SNR. The 2.5 PN waveform has the highest mass reach, being 3.5 times the mass reach of the RWF. In the equal mass case displayed in the right panel, the differences in harmonic content of different PN order waveforms are more pronounced, as odd harmonics are absent. Sources are at a luminosity distance of 3 Gpc with fixed angles given by $\theta_S = \cos^{-1}(-0.6)$, $\phi_S = 1$, $\theta_L = \cos^{-1}(0.2)$, $\phi_L = 3$.

For still higher mass values, the SNRs due to the RWF and the FWF both increase until the second harmonic fails to reach the LISA band. This is due to the overall scaling of the waveform with the total mass. At such high values, it is able to compensate both for the decreasing frequency span and the higher noise of the detector in this frequency range.

E. Effect of higher harmonics in the equal mass case

In contrast to asymmetric systems discussed so far, for systems of equal mass *all* odd harmonics are absent. Consequently, for symmetric systems the mass reach of the 2.5 PN FWF will be only 3 times the mass reach of the RWF. Further, from the right panel of Fig. 4, it is clear that the 0.5 PN and the 0 PN, or RWF, are identical, as are the 1 PN and 1.5 PN waveforms. Thus the decrease in SNR for the higher PN order waveforms with increasing total mass is more pronounced than in the unequal-mass case. We also note that for masses for which the second harmonic fails to reach the detector bandwidth, the 2 PN waveform has a lower SNR than the 2.5 PN waveform. This can be explained by noting that for these masses only the fourth and sixth harmonics enter the LISA bandwidth. The 2 PN waveform contains the leading term of the fourth harmonic at 1 PN and its 2 PN correction, which interfere destructively. However, inclusion of the 2.5 PN amplitude correction leads to a constructive interference term between the 2.5 PN correction and the 1 PN term which is responsible for increasing the SNR for the 2.5 PN waveform.

It is interesting to note that the computation of the 3 PN GW polarization which will introduce a harmonic at 8Ψ will be quantitatively more significant for the equal mass case as the mass reach will be better by 33% relative to the 2.5 PN FWF as opposed to the unequal mass case where it is only 14%. This provides one motivation for work in progress towards the computation of the 3 PN accurate GW polarizations [29].

F. Variation with mass ratio

Since the mass reach depends only on the total mass, the trends remain the same for different values of mass ratios. Figure 2 compares the variation of SNRs with mass for mass ratios of 0.1 and 0.01. If the SNR is dominated by the second harmonic, the SNR is smaller for more asymmetric systems by an overall factor of ν, where $\nu = m_1 m_2/m^2$. However, once the second harmonic fails to reach the sensitive bandwidth of LISA, the more asymmetric systems have a dominant contribution from the odd harmonics which scale by a further factor of $\sqrt{1-4\nu}$, which is larger for more asymmetric systems. Thus the decrease in SNR for the FWF with an increase in the total mass is less steep for more asymmetric systems.

G. Distance reach with the 2.5 PN FWF

Next, we compare the distance reach of the RWF and the 2.5 PN FWF. The results are shown graphically in Fig. 5

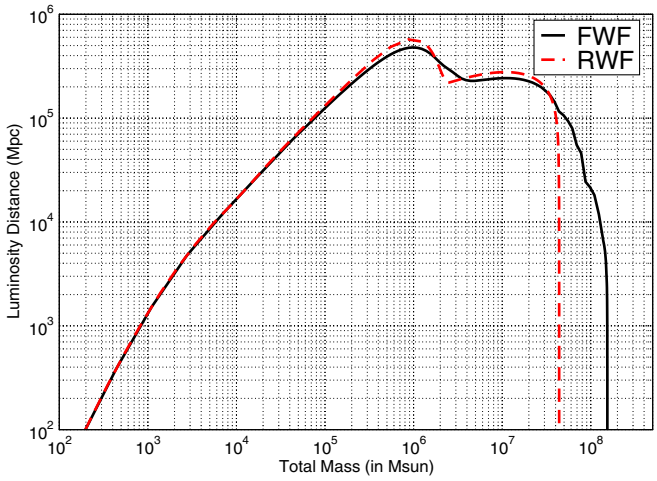

FIG. 5 (color online). Luminosity distance (in Mpc) versus total mass for a fixed SNR of 10. The systems have mass ratio of 0.1. The distance reach can be as large as 500 Gpc for systems where the second harmonic enters the LISA bandwidth. Systems undetectable by the RWF (of mass around $10^8 M_\odot$) can be detected by the FWF at distances up to 10 Gpc. The location and orientation of the sources are the same as in the earlier figures.

and are similar in appearance to the mass-reach plot. The mass reach of the RWF is $\simeq 4 \times 10^7 M_\odot$. For a system of total mass $5 \times 10^7 M_\odot$, the plot shows that LISA can detect such binaries with an SNR of 10 at a luminosity distance of 100 Gpc ($z \simeq 15$). SMBHs of total mass $\sim 10^8 M_\odot$, not even observable using RWF templates, have a distance reach as high as 10 Gpc ($z \simeq 1.5$) with an SNR of 10.

Proposals to extend the frequency bandwidth of LISA up to 10^{-5} Hz have been discussed. In that case, the FWF can increase the mass reach of LISA to even around $10^9 M_\odot$. More specifically, LISA can then observe a $10^9 M_\odot$ system with an SNR of about 30 at 3 Gpc, if it uses templates based on the 2.5 PN FWF for data analysis.

H. Sensitivity of SNR to source location and orientation

All the results for SNR using the amplitude-corrected waveforms quoted earlier in this paper have been for a fixed choice of location and orientation of the source [defined by the angles $(\theta_S, \phi_S, \theta_L, \phi_L)$] with respect to the barycenter coordinate system. To conclude our present analysis, in this section we look into the variation in the value of SNR for sources at various locations in the sky and various orientations. To this end, we consider a collection of sources randomly oriented in the sky and study the probability distribution of their SNRs. The results of our simulations (consisting of 8000 random realizations of the angles involved) are shown in Fig. 6. From the left panel of Fig. 6 we see that the most-probable SNR due to the FWF for a $(10^5, 10^6) M_\odot$ binary is less than the most-probable SNR due to the RWF, indicating that this trend is independent of the source location and orientation. In the right panel we see that a binary of mass $2 \times (10^6, 10^7) M_\odot$,

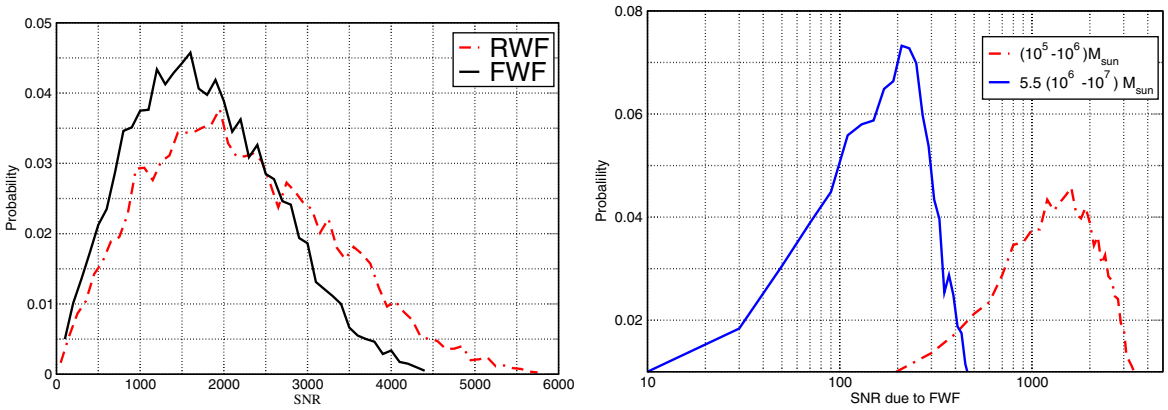

FIG. 6 (color online). Distribution of SNR with sources randomly located and oriented in the sky. The left figure plots SNRs due to both RWF and FWF for a binary of mass $(10^5 - 10^6)M_\odot$. For this mass, the most-probable SNR for the FWF is lower than the most-probable SNR for the RWF, like the trend shown in Table I. The right figure compares the SNRs due to the FWF for binaries of mass $(10^5 - 10^6)M_\odot$ and $5.5(10^6 - 10^7)M_\odot$.

which is undetectable by the RWF, can be observed by the FWF with a most-probable SNR of around 220.

V. SUMMARY

The implications of amplitude-corrected 2.5 PN FWFs for the construction of detection templates for LISA are investigated in detail. With the FWF, LISA can observe sources which are favored by astronomical observations, but not observable with RWFs. This includes binaries in the mass range 10^8–$10^9 M_\odot$, depending on whether the lower cutoff for LISA is chosen to be at 10^{-4} Hz or 10^{-5} Hz. With an SNR of 10, these systems can be observed up to a redshift of about 1.5. The computation of the 3 PN polarization, which will introduce a harmonic at 8Ψ (i.e. 4 times the dominant harmonic), in addition to the existing harmonics, could enhance the mass reach for equal mass binaries by 33% and unequal mass binaries by 14.3%.

The implication of the FWF for parameter estimation will be far more important than the extension of LISA's mass reach reported here. From the work of Van Den Broeck and Sengupta in the context of ground-based detectors [24] it is already clear that most parameters will be estimated with errors $\sim$ 10 times smaller as compared to RWF. This raises the interesting possibility that binary SMBH coalescences might be located on the sky with accuracies good enough for optical observations to identify the galaxy cluster and measure its redshift. Needless to say that this improved estimation of source properties will have important consequences in shedding light on the dark energy, better understanding of SMBH formation and evolution, structure formation, etc., and is currently under investigation.

In this work we have confined ourselves to only non-spinning black holes ignoring the effect of spin-orbit coupling at 1.5 PN [30] and 2.5 PN [31] and spin-spin effect at 2 PN order [32]. The effect of spin is expected to be astrophysically significant and it is important to revisit the present analysis including spin in the future. Though partial results for GW polarizations including spin do exist, a more exhaustive exercise would be necessary before the FWF required for this work is available. The problem will also be more complicated due to modulations arising from spin-orbit and spin-spin couplings which would need to be addressed.

In this work we also restricted to the inspiral phase and used a physical picture of the LSO that is based on the test-particle limit. For comparable masses, the notion of LSO is not as sharp, or unique, and hence our results are probably idealized limits of the real situation. Numerical relativity [33–35] is maturing over the past couple of years and could soon provide waveforms for late inspiral and merger. It should then be possible to compare the results of such numerical templates with those studied in this paper to provide a better understanding of how higher harmonics facilitate the mass reach of our detectors.

ACKNOWLEDGMENTS

K. G. A. acknowledges the Cardiff University for hospitality during the initial stages of this work and thanks Chris Van Den Broeck and Anand Sengupta for useful discussions on data analysis with the FWF for ground-based detectors. K. G. A. also acknowledges VESF. B. R. I., B. S. S., and S. S. thank the Institut Henri Poincaré and B. R. I. the Institut des Hautes Etudes Scientifiques for hospitality during the initial stages of this work. All the calculations reported in this paper are performed with *Mathematica*.

[1] L. Ferrarese and D. Merritt, Astrophys. J. **539**, L9 (2000).
[2] D. Richstone, E. A. Ajhar, R. Bender, G. Bower, A. Dressler, S. M. Faber, A. V. Filippenko, K. Gebhardt, R. Green, L. C. Ho, *et al.*, Nature (London) **395**, A14 (1998).
[3] S. Komossa *et al.*, Astrophys. J. **582**, L15 (2003).
[4] http://lisa.jpl.nasa.gov.
[5] S. A. Hughes, Mon. Not. R. Astron. Soc. **331**, 805 (2002).
[6] E. Berti, A. Buonanno, and C. M. Will, Phys. Rev. D **71**, 084025 (2005).
[7] E. Berti, A. Buonanno, and C. M. Will, Classical Quantum Gravity **22**, S943 (2005).
[8] K. G. Arun, B. R. Iyer, M. S. S. Qusailah, and B. S. Sathyaprakash, Classical Quantum Gravity **23**, L37 (2006).
[9] K. G. Arun, B. R. Iyer, M. S. S. Qusailah, and B. S. Sathyaprakash, Phys. Rev. D **74**, 024025 (2006).
[10] S. A. Hughes and K. Menou, Astrophys. J. **623**, 689 (2005).
[11] C. Cutler *et al.*, Phys. Rev. Lett. **70**, 2984 (1993).
[12] L. Blanchet, G. Faye, B. R. Iyer, and B. Joguet, Phys. Rev. D **65**, 061501(R) (2002); **71**, 129902(E) (2005).
[13] L. Blanchet, T. Damour, G. Esposito-Farèse, and B. R. Iyer, Phys. Rev. Lett. **93**, 091101 (2004).
[14] C. Cutler, T. Apostolatos, L. Bildsten, L. Finn, E. Flanagan, D. Kennefick, D. Markovic, A. Ori, E. Poisson, G. Sussman, *et al.*, Phys. Rev. Lett. **70**, 2984 (1993).
[15] C. Cutler and E. Flanagan, Phys. Rev. D **49**, 2658 (1994).
[16] L. Blanchet, T. Damour, B. R. Iyer, C. M. Will, and A. G. Wiseman, Phys. Rev. Lett. **74**, 3515 (1995).
[17] L. Blanchet, Phys. Rev. D **54**, 1417 (1996); **71**, 129904(E) (2005).
[18] L. Blanchet, B. R. Iyer, C. M. Will, and A. G. Wiseman, Classical Quantum Gravity **13**, 575 (1996).
[19] K. G. Arun, L. Blanchet, B. R. Iyer, and M. S. S. Qusailah, Classical Quantum Gravity **21**, 3771 (2004); **22**, 3115 (2005).
[20] A. M. Sintes and A. Vecchio, in *Rencontres de Moriond:Gravitational Waves and Experimental Gravity*, edited by J. Dumarchez (Frontières, Paris, 2000).
[21] A. M. Sintes and A. Vecchio, in *Third Amaldi conference on Gravitational Waves*, edited by S. Meshkov, American Institute of Physics Conference Series (American Institute of Physics, New York, 2000), p. 403.
[22] C. Van Den Broeck, Classical Quantum Gravity **23**, L51 (2006).
[23] C. Van Den Broeck and A. Sengupta, Classical Quantum Gravity **24**, 155 (2007).
[24] C. Van Den Broeck and A. S. Sengupta, Classical Quantum Gravity **24**, 1089 (2007).
[25] C. Cutler, Phys. Rev. D **57**, 7089 (1998).
[26] T. Damour, B. R. Iyer, and B. S. Sathyaprakash, Phys. Rev. D **62**, 084036 (2000).
[27] J. G. Baker and J. Centrella, Classical Quantum Gravity **22**, S355 (2005).
[28] K. G. Arun, Phys. Rev. D **74**, 024025 (2006).
[29] L. Blanchet, G. Faye, B. R. Iyer, and S. Sinha (work in progress).
[30] L. Kidder, C. Will, and A. Wiseman, Phys. Rev. D **47**, R4183 (1993).
[31] L. Blanchet, A. Buonanno, and G. Faye, Phys. Rev. D **74**, 104034 (2006); **75**, 049903(E) (2007).
[32] E. Poisson and C. Will, Phys. Rev. D **52**, 848 (1995).
[33] B. Bruegmann, W. Tichy, and N. Jansen, Phys. Rev. Lett. **92**, 211101 (2004).
[34] F. Pretorius, Phys. Rev. Lett. **95**, 121101 (2005).
[35] J. G. Baker, J. Centrella, D.-I. Choi, M. Koppitz, and J. van Meter, Phys. Rev. D **73**, 104002 (2006).